condensed matter

Article

Influence of Anharmonic and Frustration Effects on Josephson Phase Qubit Characteristics

Iman N. Askerzade [1,2]

[1] Department of Computer Engineering and Center of Excellence of Superconductivity Research, Ankara University, Ankara TR06100, Turkey; imasker@eng.ankara.edu.tr; Tel.: +90-3122033300 (ext. 1750)
[2] Institute of Physics Azerbaijan National Academy of Sciences, H.Cavid 33., AZ1143 Baku, Azerbaijan

Abstract: This study is devoted to the investigation of the Josephson phase qubit spectrum considering the anharmonic current-phase relation of the junction. The change in energy difference in the spectrum of phase qubits based on single-band/multiband Josephson junctions is also analyzed. It was shown that the presence of the anharmonic term in the current-phase relation and frustration effects in the junction electrodes leads to changing effective plasma frequencies in the different cases and results in an energy spectrum.

Keywords: phase qubit; current-phase relation; frustration; anharmonism

check for updates

Citation: Askerzade, I.N. Influence of Anharmonic and Frustration Effects on Josephson Phase Qubit Characteristics. *Condens. Matter* **2023**, *8*, 20. https://doi.org/10.3390/condmat8010020

Academic Editors: Ali Gencer, Annette Bussmann-Holder, J. Javier Campo Ruiz and Valerii Vinokur

Received: 16 November 2022
Revised: 4 February 2023
Accepted: 6 February 2023
Published: 9 February 2023

1. Introduction

In contrast to classical computation, in quantum computation we have quantum mechanical operations on the input state to derive an output [1]. It is well known that a qubit is the basic element of a quantum computer. For the study of the properties of the qubits, it is necessary to solve the corresponding stationary Schrödinger equation with an appropriate boundary condition

$$H\Psi = E\Psi \tag{1}$$

where H is the Hamiltonian operator, Ψ is the wavefunction, and E is the eigenenergy. The quantum dynamical behavior of a single Josephson junction can be described using the periodical potential in the framework of the Mathieu-Bloch picture [2,3].

A phase qubit using a single Josephson junction is schematically presented in Figure 1. The Hamiltonian of this qubit has the form [4].

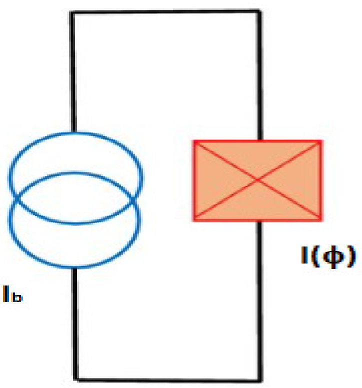

Figure 1. Schematic presentation of a phase qubit on the Josephson junction.

$$H = -E_C \frac{\partial^2}{\partial^2 \phi} - E_J\{\cos\phi + i_b\phi\} \tag{2}$$

In Equation (2): $i_b = \frac{I_b}{I_c}$ is the normalized bias current applied to the junction; I_c is the critical current of the Josephson junction; and C is the electrical capacity of the Josephson junction. Notation $E_J = \frac{\hbar I_c}{2e}$ corresponds to Josephson coupling energy, $E_C = \frac{e^2}{2C}$ is the Coulomb energy, and ϕ means the phase difference at the Josephson junction. In the case of a small bias current and the conventional current-phase relation, $I = I_c \sin\phi$, the potential energy has a form $U(\phi) = -E_J\{\cos\phi + i_b\phi\}$ (Figure 2).

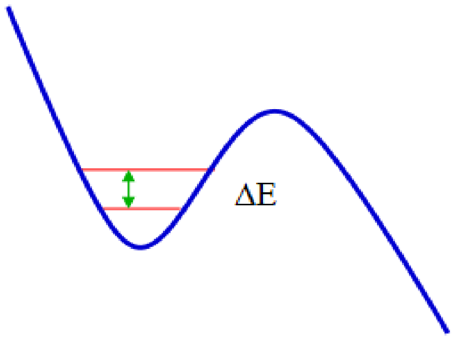

Figure 2. Profile of potential energy $U(\phi) = -E_J\{\cos\phi + i_b\phi\}$ of the Josephson phase qubit.

In this case, the energy spectrum of the phase qubit is identical to the spectrum of the harmonic oscillator [3,4]

$$E_n = \hbar\Omega_p(n + \frac{1}{2}) \tag{3a}$$

where Ω_p is the plasma frequency corresponding to phase oscillations near the minimum of potential $U(\phi)$ (Figure 2) and calculated as [2,4].

$$\Omega_p = \left(\frac{2eI_c}{\hbar C}\right)^{1/2} (1 - {i_b}^2)^{1/4} \tag{3b}$$

The energy difference between 0 and 1 levels is determined by the plasma frequency of junctions

$$\Delta E = E_1 - E_0 = \hbar\Omega_p \tag{4}$$

For the study of the Josephson dynamics, the current-phase relation of the junction is usually considered as $I = I_c \sin\phi$ [2,4]. The Josephson junction-based low-temperature superconductor reveals the sinusoidal current-phase relation. However, in the case of junctions on high-T_c superconductors, the current-phase relation includes the second term [3,5,6],

$$I = I_c f_\alpha(\phi) = I_{c0}(\sin\phi + \alpha\sin 2\phi) \tag{5}$$

where the value of parameter α is determined by the technology. In general, the value of anharmonism α in the current-phase relation is associated with the d-wave character of the superconducting gap parameter in high-T_c superconductors and multiband behavior of the superconducting state in new iron-based compounds [3,7].

In the case of Josephson junctions, when one electrode is formed by a single- and another by the multiband superconducting compound, the phase dynamics are influenced by the frustration effects [6,7]. In particular, the inclusion of the frustrated ground state in multiband superconductors leads to the φ-junction peculiarity. The influence of frustration effects in multiband compounds and Josephson junctions on these bases is studied in Refs. [8–13]. The influence of frustration effects in multiband superconductors on the escape rate in a single junction was considered in papers [14,15]. Detailed calculations of the escape rate for the ac SQUID on the junction with a generalized current-phase relation were conducted in the study [16].

As follows from Equations (3b) and (4), when the bias current approaches the critical current, level broadening due to macroscopic quantum tunneling starts to play a role [2–4]. The macroscopic quantum tunneling rate for the lowest level is given by

$$\Gamma_{MQT} = \frac{52\Omega_p}{2\pi}\sqrt{\frac{U_{\max}}{\hbar\Omega_p}}e^{-\frac{7.2U_{\max}}{\hbar\Omega_p}} \tag{6}$$

where $U_{\max} = \frac{\sqrt{2}\hbar}{e}(1 - \frac{I_e}{I_c})^{3/2}$ is the height of the potential barrier at a given bias current. This means that the relaxation and decoherence effects in phase qubits are sensitive to the intrinsic noise of the critical current of the junction [4]. The control of qubit characteristics can be tuned by the interlevel distance ΔE. From this point of view, the energy difference between levels of phase qubits ΔE on the Josephson junction based on single-/multiband superconductors and with an anharmonic current-phase relation seems interesting.

Thus, in this paper, we discuss the influence of anharmonic effects in the current-phase relation on the energy spectrum of phase qubits. We also calculate the plasma frequency and, as a result, the spectrum of phase qubits on the base of a single-/multiband Josephson junction, considering frustration effects in multiband superconductors.

2. Results

As shown in [17,18], the additional second harmonic in the current-phase relation causes the renormalization of critical current I_{c0}. For this purpose, it can be obtained by an analytical solution for the extremum point of the dependence $f_\alpha(\phi)$ (5) in a similar manner to paper [17]. The final result of the expression for the renormalized critical current at a small value α can be written as

$$\frac{I_{ceff}}{I_{c0}} = 1 + 2\alpha^2$$

As followed from the calculations, with the increased value of α, the effective critical current $\frac{I_{ceff}}{I_{c0}}$ also increased. At high values of the anharmonicity parameter α, expression (6) is converted to linear behavior. The experimental results related to the changing critical current as a function of anharmonicity parameter α are presented in Ref. [18].

For the junctions on single- and multiband junctions (in single-band/single-band case $I = I_c \sin\chi$), the Josephson current is the sum of different tunneling channel currents [14–16]

$$I = I_{c1}\sin\chi + I_{c2}\sin(\chi+\phi) + I_{c3}\sin(\chi+\theta) + \dots. \tag{7}$$

where $I_{c1,2,3,\dots}$ critical currents in the different channel, ϕ,θ, ... are the phase differences between order parameters in a frustrated state of multiband superconductor. In a single-band superconductor with the zeroes phase, we have $\Psi_0 = |\Psi_0|\exp(0)$. The multiband superconductor can be written as follows: $\Psi_1 = |\Psi_1|\exp(\chi)$, $\Psi_2 = |\Psi_2|\exp(\chi+\phi)$, $\Psi_3 = |\Psi_3|\exp(\chi+\theta), \dots$ The Ginzburg–Landau free energy functional with the multiband character of superconducting state [19–21] is true

$$F = \int d^3r(\sum_{ij}(F_{ii} - F_{ij} + \frac{H^2}{8\pi}) \tag{8}$$

where

$$F_{ii} = \frac{\hbar^2}{4m_i}\left|\left(\nabla - \frac{2\pi i\vec{A}}{\Phi_0}\right)\Psi_i\right|^2 + \alpha_i(T)|\Psi_i|^2 + \beta_i|\Psi_i|^4/2 \tag{9}$$

$$F_{ij} = \varepsilon_{ij}(\Psi_i^*\Psi_j + c.c.) + \varepsilon_1^{ij}\left\{\left(\nabla + \frac{2\pi i\vec{A}}{\Phi_0}\right)\Psi_i^*\left(\nabla - \frac{2\pi i\vec{A}}{\Phi_0}\right)\Psi_j + c.c.\right\} \tag{10}$$

m_i are the masses of the carriers in different bands, (i = 1–3); $\alpha_i = \gamma_i(T - T_{ci})$ which are linearly dependent on temperature T; β_i and $\gamma_i$are constants; $\varepsilon_{ij} = \varepsilon_{ji}$ and $\varepsilon_1{}^{ij} = \varepsilon_1{}^{ji}$ mean the interaction between superconducting gaps and their gradients, respectively; H is the external magnetic field applied to example; and Φ_0 is the magnetic flux quantum. In the case of single- and two-band junctions, for the phase differences ϕ of gap parameters, we have the effective critical current, as presented in Ref. [14].

$$I_{ceff} = (I_{c1} + I_{c2}) \text{ for } \phi = 0 \tag{11a}$$

$$I_{ceff} = (I_{c1} - I_{c2}) \text{ for } \phi = \pi \tag{11b}$$

In [15], for single-/three-band junctions, in the case of identical and positive interband interaction term $\varepsilon_{ij} = \varepsilon_{ji} = \varepsilon > 0$, the phase differences in frustration states are given as $\begin{pmatrix} \phi \\ \theta \end{pmatrix} = \begin{pmatrix} 2\pi/3 \\ -2\pi/3 \end{pmatrix}$ and $\begin{pmatrix} \phi \\ \theta \end{pmatrix} = \begin{pmatrix} -2\pi/3 \\ 2\pi/3 \end{pmatrix}$ [15]. In other possible frustration states, we have $\begin{pmatrix} \phi \\ \theta \end{pmatrix} = \begin{pmatrix} 0 \\ \pi \end{pmatrix}; \begin{pmatrix} \pi \\ 0 \end{pmatrix}$ and $\begin{pmatrix} \phi \\ \theta \end{pmatrix} = \begin{pmatrix} \pi \\ \pi \end{pmatrix}$. From the expression for the potential energy of single-/three-band junctions $U(\phi)$, we can get effective critical current

$$I_{ceff} = I_{c1}\left((1 - \frac{I_{c2}}{2I_{c1}} - \frac{I_{c3}}{2I_{c1}})^2 + (\frac{I_{c3}}{I_{c1}} - \frac{I_{c2}}{I_{c1}})^2 \right)^{1/2} \tag{12}$$

In the derivation of the last equation, it was found that the Josephson junction reveals the φ-junction peculiarity $I = I_{ceff} \sin(\phi - \varphi)$, with $\varphi = \arctan\frac{I_{c3} - I_{c2}}{I_{c1} - \frac{I_{c2}}{2} - \frac{I_{c3}}{2}}$. In the other frustration state $\begin{pmatrix} \phi \\ \theta \end{pmatrix} = \begin{pmatrix} -2\pi/3 \\ 2\pi/3 \end{pmatrix}$, the terms I_{c2} and I_{c3} in Equation (12) were replaced by the places. The frustration case $\begin{pmatrix} \phi \\ \theta \end{pmatrix} = \begin{pmatrix} 0 \\ \pi \end{pmatrix}$ corresponds to the effective critical current

$$I_{ceff} = (I_{c1} + I_{c2} - I_{c3}) \tag{13}$$

In the $\begin{pmatrix} \phi \\ \theta \end{pmatrix} = \begin{pmatrix} \pi \\ \pi \end{pmatrix}$ state, we have the following expression for the effective critical current:

$$I_{ceff} = (I_{c1} - I_{c2} - I_{c3}) \tag{14}$$

3. Discussion

Quantum computation for using Josephson phase qubits needs to use a working temperature at the level mK [1–3]. The low-temperature anharmonic character of the current-phase relation becomes important and, as a result, this effect must be considered in the realization to phase qubits [3–5]. Using numerical calculations for the effective critical current in Equation (5) leads to the results for the energy differences between 0 and 1 levels in phase qubits, which are presented in Figure 3 $\alpha < 0.5$. The $\alpha > 0.5$ second term in Equation (5) becomes dominant and the effective critical current is determined by this term. The increase of $\Delta E/\Delta E_0$ (ΔE_0 is the energy difference in the harmonic case) results in the increase of anharmonicity parameter α.

The numerical results for the normalized ratio $\Delta E/\Delta E_0$ (ΔE_0 is the energy distance of single-/single-band junction) in a single-/two-band junction-based qubit versus I_{c2}/I_{c1} is presented in Figure 4. As can be seen, the ΔE_0 (I_{c2}/I_{c1}) dependence reveals the increasing character at $\phi = 0$. The calculations of ΔE_0 (I_{c2}/I_{c1}) in the limit $\phi = \pi$ are also plotted in Figure 4 and reveal the opposite character to the case $\phi = 0$.

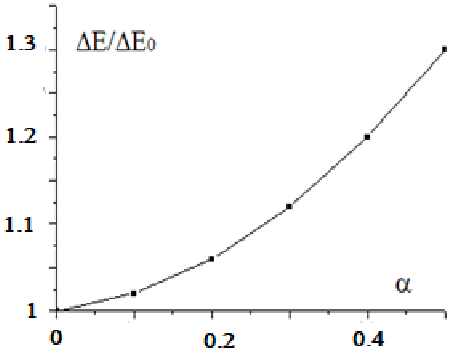

Figure 3. Changing the energy difference between levels $\Delta E/\Delta E_0$ versus anharmonicity.

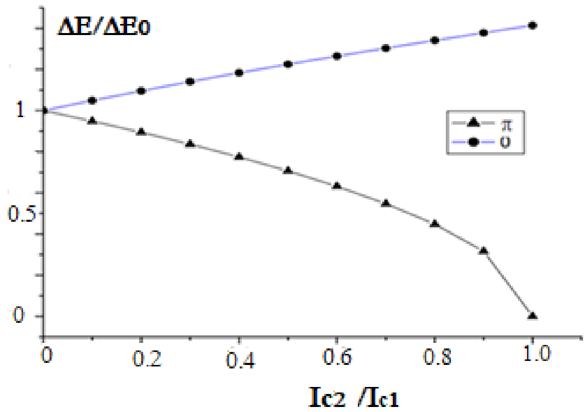

Figure 4. Changing the energy difference between levels $\Delta E/\Delta E_0$ in qubit based on the single-/two-band junction versus I_{c2}/I_{c1}.

The variations of the ratio $\Delta E/\Delta E_0$ versus I_{c3}/I_{c1} in the case of single-band/three-band junction-based qubits are plotted in Figure 5 in the frustration state $\begin{pmatrix} \phi \\ \theta \end{pmatrix} = \begin{pmatrix} -2\pi/3 \\ 2\pi/3 \end{pmatrix}$ for different values of I_{c2}/I_{c1} = 0, 0.5, 1 (from top to bottom). The changing character of the ratio $\Delta E/\Delta E_0$ results in increasing the ratio I_{c3}/I_{c1}. At high values of I_{c2}/I_{c1} = 1, we have the behavior similar to the single-band/two-band case with the opposite phase difference $\phi = \pi$. The ratio $\Delta E/\Delta E_0$ reveals a minimum in the case of low values of the ratio I_{c2}/I_c = 0, 0.5. In the frustration case, $\begin{pmatrix} \phi \\ \theta \end{pmatrix} = \begin{pmatrix} 0 \\ \pi \end{pmatrix}$ and $\begin{pmatrix} \phi \\ \theta \end{pmatrix} = \begin{pmatrix} \pi \\ \pi \end{pmatrix}$, using the effective critical current (see Equations (13) and (14)), has a form similar to Figure 4 in the case of a single-/two-band structure.

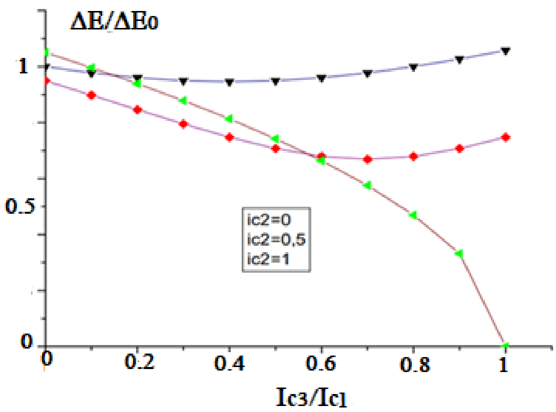

Figure 5. Changing the energy difference between levels in qubit based on single-/three-band junction $\Delta E/\Delta E_0$ versus I_{c3}/I_{c1} for I_{c2}/I_{c1} = 0, 0.5, 1 (from top to bottom).

It is useful to note that no direct observation of the change in $\Delta E/\Delta E_0$ phase qubits is based on single-/multiband junctions. However, there is experimental evidence of a decreasing critical current in the case of single–/two-band junctions with positive interband interaction parameters. In Ref. [22], single-/three-band junction was investigated, and it described the effects of the asymmetric critical current, Shapiro steps. The effect of the asymmetrical critical current has been observed in the edge-type junction between PbIn and many-band Co-doped $BaFe_2As_2$ thin film, as presented in Ref. [23]. In such junctions, a critical voltage I_cR_N of about 12 μV. In Ref. [24], the junction between *PbIn* and the $Ba_{1-x}K_x(FeAs)_2$ x = 0.29 and 0.49 was realized. In this study, it was studied experimentally as a PbIn/BaK$(FeAs)_2$ point-contact junction. It was also theoretically shown that the three-band superconducting state scenario provides better results for the treatment of the observed data. In papers [25,26], Nb/BaNa$(FeAs)_2$ junctions were reported with very a small critical voltage I_cR_N, approximately 3 μV. This fact can be explained by the cancellation of the opposite supercurrents in the frustrated state of multiband iron-based superconductors. The reduction of the Josephson plasma frequency in such three-band structures was also obtained by the theoretical investigation in paper [27]. We hope that the obtained theoretical results for changing $\Delta E/\Delta E_0$ phase qubits will be observed experimentally.

4. Conclusions

In this study, the energy difference between the levels of phase qubits on the Josephson junction, based on single-/multiband superconductors, was calculated. It was shown that, in all cases, the frustration effects in multiband superconductors lead to a change in energy difference between levels $\Delta E/\Delta E_0$. The change $\Delta E/\Delta E_0$ is determined by the value of the critical currents in different channels. The phase qubit on the junction with anharmonic current-phase relation $\Delta E/\Delta E_0$ increases with an increase in the amplitude of the second term.

Funding: This study is partially supported by the TÜBİTAK grant No. 118F093.

Data Availability Statement: Not applicable.

Conflicts of Interest: The author declares no conflict of interest.

References

1. Nielsen, M.; Chiang, I. *Quantum Computation, Quantum Information*; Cambridge University Press: Cambridge, UK, 2000; 676p.
2. Likharev, K. *Introduction into Dynamics of Josephson Junctions and Circuits*; Gordon Breach: New York, NY, USA, 1986; 586p.
3. Askerzade, I.; Bozbey, A.; Canturk, M. *Modern Aspects of Josephson Dynamics and Superconductivity Electronics*; Springer: Berlin, Germany, 2017; 211p. [CrossRef]
4. Wendin, G.; Shumeiko, V. Quantum bits with Josephson junctions. *Low Temp. Phys.* **2007**, *33*, 724–757. [CrossRef]
5. Il'ichev, V.; Zakosarenko, I.; Fritzsch, L.; Stolz, R.; Hoenig, H.E.; Meyer, H.-G. Radio-frequency based monitoring of small supercurrents. *Rev. Sci. Instrum.* **2001**, *72*, 1882–1922. [CrossRef]
6. Yerin, Y.; Omelyanchouk, A.N. Frustration phenomena in Josephson point contacts between single-band and three-band superconductors. *Low Temp. Phys.* **2014**, *40*, 943–949. [CrossRef]
7. Askerzade, I. *Unconventional Superconductors: Anisotropy and Multiband Effects*; Springer: Berlin, Germany, 2012; 177p.
8. Yerin, Y.; Omelyanchouk, A.N.; Il'Ichev, E. DC SQUID based on a three-band superconductor with broken time-reversal symmetry. *Supercond. Sci. Technol.* **2015**, *28*, 095006. [CrossRef]
9. Ng, T.; Nagaosa, N. Broken time-reversal symmetry in Josephson junction involving two-band superconductors. *EPL* **2009**, *87*, 17003. [CrossRef]
10. Stanev, V.; Tešanović, Z. Three-band superconductivity and the order parameter that breaks time-reversal symmetry. *Phys. Rev. B* **2010**, *81*, 134522. [CrossRef]
11. Dias, R.; Marques, A. Frustrated multiband superconductivity. *Supercond. Sci. Technol.* **2011**, *24*, 085009. [CrossRef]
12. Lin, S.-Z. Josephson effect between a two-band superconductor with s++ or s± pairing symmetry and a conventional s-wave superconductor. *Phys. Rev. B* **2012**, *86*, 014510. [CrossRef]
13. Bojesen, T.; Babaev, E.; Sudbø, A. Time reversal symmetry breakdown in normal and superconducting states in frustrated three-band systems. *Phys. Rev. B* **2013**, *88*, 220511. [CrossRef]
14. Askerzade, I.N. Escape rate in Josephson junctions between single -band and two -band superconductors. *Physical C* **2020**, *374*, 1353647. [CrossRef]

15. Askerzade, I.N.; Aydın, A. Frustration effect on escape rate in Josephson junctions between single-band and three-band superconductors in the macroscopic quantum tunneling regime. *Low Temp. Phys.* **2021**, *47*, 282–286. [CrossRef]
16. Askerzade, I.N.; Askerbeyli, R.; Ulku, I. Effect of unconventional current-phase relation of Josephson junction on escape rate in ac SQUID. *Physical C* **2022**, *598*, 1354068. [CrossRef]
17. Goldobin, E.; Koelle, D.; Kleiner, R.; Buzdin, A. Josephson junctions with second harmonic in the current-phase relation: Properties of φ- junctions. *Phys. Rev. B* **2007**, *76*, 224523. [CrossRef]
18. Bauch, T.; Lombardi, F.; Tafuri, F.; Barone, A.; Rotoli, G.; Delsing, P.; Claeson, T. Macroscopic quantum tunneling in d-wave YBCO Josephson junctions. *Phys. Rev. Lett.* **2005**, *94*, 087003. [CrossRef]
19. Askerzade, I.; Gencer, A.; Guclu, N. On the Ginsburg-Landau analysis of the upper critical field H-c2 in MgB2, Supercond. *Sci. Technol.* **2002**, *15*, L13–L16. [CrossRef]
20. Askerzade, I.; Gencer, A.; Guclu, N.; Kılıc, A. Two-band Ginzburg-Landau theory for the lower critical field H-c1 in MgB2, Supercond. *Sci. Technol.* **2002**, *15*, L17–L20. [CrossRef]
21. Askerzade, I. Study of layered superconductors in the theory of an electron-phonon coupling mechanism. *Phys. Uspekhi* **2006**, *49*, 977–988. [CrossRef]
22. Döring, S.; Schmidt, S.; Schmidl, F.; Tympel, V.; Haindl, S.; Kurth, F.; Iida, K.; Mönch, I.; Holzapfel, B.; Seidel, P. Edge-type Josephson junctions with Co-doped Ba-122 thin filmsSuper. *Sci. Technol.* **2012**, *25*, 084020. [CrossRef]
23. Zhang, X.H.; Oh, Y.S.; Liu, Y.; Yan, L.; Kim, K.H.; Greene, R.L.; Takeuchi, I. Observation of the Josephson Effect in Pb/BaKaFeAs Single Crystal Junctions. *Phys. Rev. Lett.* **2009**, *102*, 147002. [CrossRef]
24. Burmistrova, A.V.; Devyatov, I.A.; Golubov, A.A.; Yada, K.; Tanaka, Y.; Tortello, M.; Gonnelli, R.S.; Stepanov, V.A.; Ding, X.; Wen, H.-H.; et al. Josephson current in Fe-based superconducting junctions: Theory and experiment. *Phys. Rev. B* **2015**, *91*, 214501. [CrossRef]
25. Kalenyuk, A.A.; Pagliero, A.; Borodianskyi, E.A.; Kordyuk, A.A.; Krasnov, V.M. Phase-Sensitive Evidence for the Sign-Reversal $s\pm$ Symmetry of the Order Parameter in an Iron-Pnictide Superconductor Using Nb/$Ba_{1-x}Na_xFe_2As_2$ Josephson Junctions. *Phys. Rev. Lett.* **2018**, *120*, 067001. [CrossRef] [PubMed]
26. Kalenyuk, A.A.; Borodianskı, A.; Kordyuk, A.A.; Krasnov, V.M. Influence of the Fermi surface geometry on the Josephson effect between iron-pnictide and conventional superconductors. *Phys. Rev. B* **2021**, *103*, 214507. [CrossRef]
27. Ota, Y.; Machida, M.; Koyama, T.; Aoki, H. Collective modes in multiband superfluids and superconductors: Multiple dynamical classes. *Phys. Rev. B* **2011**, *83*, 060507. [CrossRef]